WADC TECHNICAL REPORT 59-300
PART II

RESEARCH AND DEVELOPMENT SERVICES LEADING TO THE CONTROL OF ELECTRICAL PROPERTIES OF MATERIALS FOR HIGH TEMPERATURE RADOMES

Leon M. Atlas
Hikaru Nagao

Armour Research Foundation
of Illinois Institute of Technology

OCTOBER 1960

Materials Central
Contract No. AF 33(616)-5929
Project No. 7371

WRIGHT AIR DEVELOPMENT DIVISION
AIR RESEARCH AND DEVELOPMENT COMMAND
UNITED STATES AIR FORCE
WRIGHT-PATTERSON AIR FORCE BASE, OHIO

800 — January 1961 — 15-693C

FOREWORD

This report describes the second year of a research program instituted under Air Force Contract No. AF 33(616)-5929, Project No. 7371 "Applied Research in Electrical, Electronic and Magnetic Materials," Task No. 73710 "Applied Research on Dielectric Materials." Administration of the program was under the direction of the Materials Central with Lt. J. D. Latva as task engineer.

Preparation of materials and specimens as well as the analysis of electrical data presented in the report were carried out at Armour Research Foundation of Illinois Institute of Technology, Chicago 16, Illinois. Personnel associated with this portion of the program were Dr. Leon M. Atlas, project leader, Mr. Hikaru Nagao, who carried out the statistical calculations, and Messrs. Ross F. Firestone and William K. Sumida, who aided in the preparation of specimens.

Electrical measurements were performed under the direction of Mr. W. B. Westphal on Air Force Contract No. AF 33(616)-5920 at the Laboratory for Insulation Research of Massachusetts Institute of Technology.

ABSTRACT

Alumina ceramics having less than 100 ppm total impurities and densities up to about 3.67 g/cm^3 were fabricated by firing cold pressed calcined alumina hydrate in air at temperatures up to about 1960° C. These high purity specimens were supplemented by a series of deliberately contaminated ceramics prepared by introducing known concentrations of Si, Ti, Mg, Ca, Fe, and Cr into the batch. The loss tangents and dielectric constants (k') of these discs were measured at MIT in the region 10^2 to 10^6 c/s and 25 to 500° C. Statistical analysis of the resulting data was then carried out at ARF by multiple regression methods. At 10^6 c/s and 500° C tan δ was linearly related to impurity concentration with a multiple correlation coefficient of 0.93. Si ions caused the greatest rise of tan δ , and Mg, Ti, Ca, Cr, and Fe had progressively decreasing effects. In contrast, the linear correlation coefficient at 10^2 c/s was lower than that obtained from a semi-logarithmic function, which gave a value of 0.80.

Loss tangent and dielectric constant data were also used to calculate the conductivities of the specimens at 10^5 c/s, and the activation energies of conduction at 500° C were then deduced from plots of log σ vs 1/T. In almost every case a value in the range 1.2 to 1.6 ev was obtained. Comparison with trapping energies calculated from glow curves suggests that electrons associated either with Si or Ti impurity sites were the predominant charge carriers. However, in discs doped with Mg^{2+}, the activation energy rose to 2 ev. Glow curve calculations indicate that Mg^{2+} creates traps with a depth of about 2.9 ev; therefore, Mg ions contributed significantly to the reservoir of charge carriers.

Replotting the tan δ and k' data into curves of k'' vs. frequency reveals small peaks which have been attributed to interfacial polarization controlled by grain boundaries. Using the known electrical measuring potential and the microscopically determined grain diameters, an estimated carrier mobility of 11-15 cm^2/volt sec at 25° C was calculated.

With the objective of further reducing the small positive temperature coefficient of k' of alumina, ceramics were prepared with a compensating titanate phase. Mixtures containing 90% Al_2O_3 and 10% $CaTiO_3$ were found to have an invariant dielectric constant of 11.4 to 11.7 up to 250° C at 10^7 c/s. At this frequency, the loss tangent of the two phase ceramic at 500° C is lower than that of Pyroceram 9606.

PUBLICATION REVIEW

This report has been reviewed and is approved.

FOR THE COMMANDER:

WILLIAM G. RAMKE
Chief Ceramics and Graphite Branch
Metals and Ceramics Laboratory
Materials Central

TABLE OF CONTENTS

LIST OF TABLES

LIST OF ILLUSTRATIONS

LIST OF ILLUSTRATIONS (cont'd)

I. INTRODUCTION

During its first year, the alumina dielectric program was primarily concerned with the production of alumina ceramics both of high purity, and containing known low concentrations of foreign ions. Batches were prepared by the solution of 99.999% pure metal in HCl followed by precipitation of alumina hydrate with ammonia. After being calcined at 1000 to 1300° C, this batch was formed into ceramic discs by cold pressing at 15,000 to 20,000 psi and firing at temperatures up to about 1900° C in a furnace open to the atmosphere. The resulting ceramics had a maximum density of 3.6 to 3.7 g/cm^3 and an impurity content below 100 ppm. Toward the end of the year Ca, Si, and Fe impurities were being introduced into some of the specimens by milling $CaCO_3$, SiO_2, and Fe_2O_3 into the batches.

In a parallel research program the thermoluminescence (glow curves) of the "pure" and doped aluminas - preactivated by gamma radiation - was studied. Data for specimens containing Ca, Si, and Fe - including calculated trap energies - were obtained and included in WADC Technical Report 59-300.

The second year of the program continued the fabrication of doped alumina ceramics containing Mg, Ti, and Cr as new impurity ions. Furthermore, all of the compositions were also formed into cylindrical specimens for microwave measurements in wave guides.

The objective behind the preparation of this series of "pure" and contaminated ceramic specimens was the isolation of the effects produced by each common impurity ion on the dielectric properties of alumina. This information was statistically deduced from measurements of tan δ and dielectric constant (k') performed at the Laboratory for Insulation Research of MIT in the range 10^2 to 10^7 cycles per second and 25 to 500° C. Early in the project it was found that close control of chemical composition entailed excessive time and many wasted specimens. Contamination was a serious problem and high temperature evaporation losses also contributed to the indeterminacy of the final composition of the ceramics. Consequently, it was decided to accept whatever composition came from the furnace and analyze the electrical data by multiple regression methods. Although this approach prevented the use of optimum experimental designs and limited the study of interactions, the direct effect produced by each impurity could still be effectively determined.

In addition to the rather direct statistical studies, the electrical measurements were also considered more obliquely with the result that

---

Manuscript released by the authors July 1960 for publication as a WADC Technical Report.

relationships were found between the depths of traps associated with Si, Ti and Mg sites and the activation energies of conduction at 10^5 c/s and 500° C. Furthermore, polarization peaks appearing in the k'' vs. frequency plots of some of the specimens permitted a rough estimation of carrier mobilities in polycrystalline alumina.

Disregarding dispersion effects produced by electrode barrier layers, high purity alumina was found to have nearly the same positive temperature variation of k' as far less pure commercial ceramics. Therefore, since purification alone was not effective, the problem of achieving an invarient k' was approached by the expedient of introducing a second phase having a negative temperature variation of k' into the alumina. Titanates are the most common compounds having the desired negative temperature coefficient; it only remained to choose a representative which would not react with alumina at high temperatures. Fortunately, because the titanate group is more electronegative than the aluminate, such compounds as $CaTiO_3$ and $SrTiO_3$ remain as a stable second phase when fired with alumina. Therefore it is possible to achieve a very fair compensation of k', but at the cost of appreciably raising the loss tangent.

High porosity was an ever present problem in the fabrication of high purity alumina ceramics. Fired densities slightly above 3.65 g/cm^3 (corresponding to a porosity near 9%) were the highest achieved even at firing temperatures approaching 2000° C. Much of this porosity is intragranular - a consequence of rapid crystal growth - and it appears unlikely that appreciably higher densities can be obtained without the use of additives or by means of hot pressing techniques.

II. PREPARATION OF SPECIMENS

A. Fabrication of Green Specimens

Pure alumina ceramics, and those containing low concentrations of added contaminants were prepared with calcined alumina derived from 99.999% Al metal. This high purity metal was supplied by the Reynolds Metals Company and the the British Aluminum Company, Ltd. (imported through Aluminum Transatlantic Inc.). The details of the conversion of the metal to the oxide by (a) solution in HCl, (b) precipitation with ammonia, and (c) calcination of the gelatinous alumina hydrate, have been presented in WADC Technical Report 59-300 (Ref. 1). The impurity content of the resulting alumina powder has been spectrochemically determined to be less than 100 ppm, and a typical analysis is given in Table I. The surface area of this material is variable, depending primarily on the temperature at which the hydrate is calcined. Table II shows a sharp decrease in surface area between calcining temperatures of 1100° C (51.3 $meters^2/gm$) and 1300° C (5.7 $meters^2/cm$). Note that the mean particle size does not change in a corresponding manner; this is interpreted to mean that the grains of the high surface powder are actually porous agglomerates. In an attempt to disintegrate these agglomerates, the calcined powder plus any introduced impurities (as the oxide or carbon-

ate) were wet milled with 0.5N HCl in polyethylene jars containing polystyrene balls. The pulp was then dried at about 100° C.

The calcined and milled alumina was blended with various binder solutions, including aluminum chloride, polyvinyl alcohols (DuPont Elvanol 50-42, and 70-05 in water) and an acrylic resin (Rohm and Haas Acryloid B-72 in methyl-ethyl ketone). The polyvinyl alcohol solutions were found to be effective binders and were used to prepare all of the specimens listed in Table I. The quantity of binder solution added to the alumina was varied from about 15% (corresponding to an almost dry consistency in this high surface alumina) to enough to produce a somewhat damp mass. The highest green densities were obtained with a dry consistency, but the tendency to laminate was at its worst under this condition.

Specimens varying from 1-1/4 inch to 1-7/8 inch in diameter and 3/16 inch to 3/4 inch in height were compressed under pressures of 15,000 to 100,000 psi. In an effort to obtain the highest practicable green densities from the batches calcined at 1000 to 1100° C, several consecutive pressings were used. Even under these stringent conditions, the maximum green density achieved with a powder having greater than 50 meters^2/gm was about 1.8 gm/cm^3. Evacuating the die to a pressure of four inches of mercury before and during pressing produced no discernible improvement either in green density or in the tendency to laminate.

As might be expected, the coarser alumina resulting from calcination at 1300° C could be pressed to densities of 1.8 to 2 gm/cm^3 even at pressures as low as 15,000 psi, and lamination was a much less serious problem.

B. Firing Specimen Discs

Early in the program cold pressed alumina discs were fired in an inductively heated furnace to a maximum of 1850 to 1900° C. This operation was subsequently transferred to a Zircoa gas-oxygen furnace which was capable of temperatures higher than the melting point of alumina. In this furnace, specimens were generally fired in air to a maximum temperature of 1930 to 1960° C; however, temperatures as high as 2000° C were also reached. Experiments were also carried out in which the normally oxidizing furnace atmosphere was replaced by a reducing mixture rich in carbon monoxide (51.6% CO, 34% H_2, 12% CO_2, 2% N_2, and 0.4% CH_4).

Even with these high firing temperatures, a density slightly less than 3.7 gm/cm^3 (7% porosity) was the maximum obtained with either the "pure" or doped alumina batches. Since minimum porosity is an important objective of this program, attention was recently turned to hot pressing as a fabrication method. However, because of the dielectric requirements, it is necessary to minimize the incorporation of

carbon in the specimens. Aside from the areas of direct contact between the alumina and the usual graphite dies, most of the carbon is introduced through the agency of carbon monoxide dissociation. Much of the internal carbon might therefore be eliminated by hot pressing in a vacuum or in an inert atmosphere. Preliminary experiments at 1375° C under argon have yielded alumina with a pure white interior - a sharp contrast to the characteristic gray of the usual hot pressed ceramics. Any carbonaceous residue that might occur even under argon can be removed by annealing above 1450° C in oxygen.

Another approach to densification now being pursued is the addition of powdered aluminum metal to the oxide batch. This mixture will either be hot pressed, or cold pressed and fired in an inert atmosphere, and the partly metallic sintered product will then be oxidized. This procedure should aid densification in two ways: (1) it will create oxygen deficiency defects in the alumina structure, thus accelerating sintering rates, and (2) some of the mobile aluminum may diffuse into the pores, and later oxidation will then convert the metal to the oxide.

III. ANALYSES AND PHYSICAL PROPERTIES OF ALUMINA CERAMICS

A. Physical Properties

1. Grain Size and Density

As determined by microscopic examination of polished sections, specimens fired in air at 1900 to 1940° C were composed of grains ranging from about 15 microns to 110 microns in diameter (Table III). In these specimens most of the residual porosity is at the grain boundaries and the low densities are probably due to incomplete sintering.

In contrast, introduction of carbon monoxide (or a mixed reducing gas rich in carbon monoxide) into the furnace caused a great increase in crystal growth - grain diameters of 2 mm were not uncommon. Burke (Ref. 2) has described this rapid grain enlargement as a process of secondary recrystallization which is caused by the selective growth of certain favored crystals after primary grain growth has been essentially completed. This catastrophic process is of particular importance in a high purity alumina where the absence of impurity inclusions reduces the number of obstructions to grain boundary motion, and where the initial crystallite size is very small. In specimens showing pronounced secondary recrystallization, much of the residual porosity is intragranular - engulfed by the rapidly moving grain boundaries. In this case the final density is essentially controlled by the volume of entrapped pores. These are only eliminated very slowly by the diffusion of vacancies to grain boundaries.

The above observations suggest that despite its catalytic effect on alumina sintering, CO has only limited usefulness in preparing alumina ceramics of maximum strength and density. In the absence of such a

sintering catalyst, high purity alumina densifies very slowly even at temperatures above 1900°C. If the process is allowed to continue at high temperature, secondary recrystallization will probably eventually occur even in an oxidizing atmosphere.

Density data provided by specimens fired under similar conditions in a gas-oxygen furnace (all in Table I but A7, A8, A13, and A14, which were fired in an induction furnace) show that low concentrations of most of the impurity ions exerted no significant densifying action. Surprisingly, it was only Mg - rather than Ti, Fe, or Si, which had a definite effect. This result can, however, be explained with the hypothesis that in "pure" alumina the diffusion of oxide ions is the process controlling the rate of sintering. This diffusion rate is increased by the creation of oxide ion vacancies - a consequence of introducing a divalent cation impurity such as Mg^{2+} into the corundum structure. Since TiO_2 is known to be an effective densifying agent for commercial purity aluminas, the condition must in this case be reversed: cation diffusion controls the sintering rate. This is reasonable if commercial aluminas already have high oxide ion vacancy concentrations, possibly produced by divalent impurities.

Varying the reactivity of the batch was also observed to have relatively little effect on the final density of fired ceramics (Table II). Any increase in sintering rates gained through higher surface areas was offset by the lower cold pressed densities that could be achieved. However, it is expected that high batch reactivity should be very advantageous for hot pressing.

2. Color

It was previously noted in WADC Technical Report 59-300 that many "pure" alumina ceramic specimens displayed a mottled yellow discoloration. Additions of 100 ppm of Si^{4+} to the batch, or firing in a reducing atmosphere prevented this staining, whereas Ca^{2+} or Mg^{2+} intensified it. The cause of this discoloration has been clarified by the glow curves of gamma activated specimens (Ref. 3). These curves have peaks near 90°C and 240°C attributable to Fe^{2+} (and/or Ni^{2+}) and Fe^{3+} impurities respectively. Hydrogen annealing and Si additions enhance the former and suppress the latter peak by reducing the trivalent iron to the divalent condition. Si^{4+} exerts a reducing action on polyvalent cations in alumina because of its +4 charge. In order to preserve an average +3 cationic charge, Si^{4+} will either force the creation of cation vacancies or drive such ions as Fe^{3+}, Ni^{3+} and Ti^{4+} to a lower valence state. Oxidizing atmospheres and Ca^{2+} or Mg^{2+} have the reverse effect and increase the concentration of Fe^{3+}. Since Fe^{3+} is a much more highly colored ion than Fe^{2+}, the bleaching action of Si^{4+} and CO, and the intensifying effect of divalent cations becomes understandable. The pure white color of commercial aluminas is a result of the almost universal presence of SiO_2 as a major impurity.

B. Analyses of Specimens

Spectrographic analyses were carried out at the Chicago Spectro Service Laboratory by crushing a representative ceramic of each composition between alumina blocks, diluting the powder with carbon, and introducing the mixture into carbon electrodes. Impurity concentrations were then obtained by comparison with standards, which, for the most part, were mixtures of alumina and the various impurity constituents. The accuracy of these results may be estimated by comparing the spectrographic analyses with the known concentrations of non volatile impurities introduced into some of the batches. It was found that for Si, disagreement between the two values was low, being less generally than 20% of the added concentration. On the other hand, differences ranging from $\pm$ 200 to 400% were not uncommon for Ca and Mg. Moreover, in the case of Fe, Ti, and Cr, which are volatile, analyzed concentrations were in some cases 200 to 300% higher than the quantity introduced. As a result of these discrepancies, the introduced, rather than the spectrographic concentration of Ca and Mg are presented in Table I, for batches doped with these elements. Moreover, in those cases where the analyzed concentrations of Ti, Cr, and Fe are higher than the introduced values, the latter are tabulated.

These concentration discrepancies occurring in samples with deliberately introduced impurities provide a rough measure of the accuracies that can be expected for analyses of the adventitious contaminants. The serious influence that these large analytical errors might have exerted on the correlation of electrical properties and impurity levels was diminished by the fact that the concentrations were allowed to vary by a factor of 50 or more.

Elements not reported in Table I occurred in concentrations either below 1 ppm or below the limits of detection. In the case of the more common impurities, these limits were about 10 ppm or less for Na, Mn, Ti, Ni, Co, Cr, Cu, and Ag.

IV. ELECTRICAL PROPERTIES OF "PURE" AND CONTAMINATED ALUMINA CERAMICS

A. Introduction

Determinations of tan δ and the dielectric constant were carried out at the Laboratory for Insulation Research in the range 10^2 to 10^7 c/s and 25 to 500° C. The measurements were carried out in dry nitrogen on discs averaging about 1.6 inch in diameter and 0.2 inch in thickness, and ground flat and parallel to 0.002 inch. Because of the porosity of these specimens, difficulty was encountered in depositing metal electrodes on the faces without having some absorption of the metal into the ceramic. This problem was overcome by first depositing a thin layer of carbon from an alcoholic carbon suspension, and following this with a film of aluminum. A further description of the electrical techniques as well as

curves of the temperature variation of tan δ and k' at several frequencies will be separately presented by MIT under Contract No. AF 33(616)-5920.

For the purposes of this report, some of the MIT data have been redrawn to show the frequency variation of k'' (the relative loss factor) at temperatures from 25 to 500°C (Figures 1-8), and the corresponding change in k' at 500°C (Figure 9). The replotted curves illustrate the behavior of two "pure" alumina ceramics - one annealed at 1225°C in oxygen and one in hydrogen - and a series of ceramics doped with Mg, Ca, Ti, Si, Fe, and Cr. Various aspects of these curves and of dielectric conductivity data derived from them will be discussed in detail in later sections of this report.

Dielectric losses in ceramics at low and intermediate frequencies are mainly a consequence of (1) electronic and ionic conductivity, and (2) polarization losses involved in (a) the rotation of dipoles comprised of couples or groups of ions and vacancies, and (b) the motion of charge carriers trapped within the confines of a single grain or between insulating barriers at the measuring electrodes. These mechanisms vary in importance in different regions of the tan δ -T-frequency field studied by MIT. At the higher frequencies and temperatures, electronic conductivity is the dominant loss mechanism. However, as indicated by activation energy data, this conductivity is extrinsic for even the purest of the alumina specimens at 500°C and 10^5 c/s. At low frequencies and high temperatures the importance of interfacial polarization, caused by high resistance barrier layers at the measuring electrodes (Ref. 4), is suggested by the very marked dispersion of k'. At lower temperatures, the contribution of grain boundary resistance to interfacial polarization (Refs. 5, 6) might be the cause of the low maxima in several of the k'' vs. f curves of Figures 1, 2 and 5. Alternatively, these peaks may have their origin in ionic relaxation phenomena of the type described by Breckenridge (Ref. 7). At low frequencies ionic conductivity is also an important source of dielectric losses.

B. Statistical Correlation of Impurity Concentration and Loss Tangent

Table IV presents the loss tangents of twenty two alumina ceramics at 500°C, and 10^6 and 10^2 c/s. The relationship between these values and the compositions listed in Table I were analyzed by multiple regression (Ref. 8) - a method which attempts to reduce the data to a single equation preferably of the simple form:

$$Y_o = b_1 x_1 + b_2 x_2 + b_3 x_3 + \ldots + A \qquad (1)$$

In the present program Y_o is tan δ at 500°C and 10^6 c/s or 10^2 c/s; $x_1, x_2, \ldots, x_5$ are the concentrations of Si, Ti, Mg, Ca, and Fe; $b_1, b_2, \ldots, b_5$ are the slope constants or partial regression coefficients of the concentration variables, and A is the intercept constant. Evaluation of the partial regression coefficients permits (a) a prediction of

tan δ for interpolated concentrations of any one or more impurities, and (b) a comparison (by means of the standardized partial regression coefficients) of the importance of each impurity. In addition, the intercept A provides an estimate of the loss tangent of a ceramic containing an impurity concentration of zero. Since Equation (1) is linear, and the relationship between dependent and independent variables is in practice not always so simple, it is sometimes necessary to allow the x's to represent functions of the measured quantities. Moreover, it is not always true that the x's independently influence Y_o. In this case, interactions between the x's necessitate additional terms (such as cross products) beyond those which describe the direct effects of each independent variable. The benefit of these refinements of Equation (1) is demonstrated by rising values of R (the multiple correlation coefficient) as each is introduced.

1. 10^6 Cycles Per Second

At 500° C and 10^6 c/s, a value of R = 0.93 was obtained for the simple linear relationship of Equation (1) with no interaction terms. Since activation energy data show that the losses in this region are primarily due to extrinsic electronic conduction, the linearity corroborates the fact that each impurity ion introduces a fixed number of defects, which in turn activate a definite number of electrons or holes. The straight lines given by the solution of the regression equation are shown in Figure 10. In this figure the line for chromium was not obtained by regression because of a lack of sufficient concentration values. For this impurity, therefore, the separate effects of Si, Ti, Ca, Mg, and Fe were first multiplied by their concentrations in specimens A60 and A61, and the results were subtracted from the measured loss tangents at 10^6 c/s and 500° C. The residual losses were then considered to reflect the influence of Cr.

Actually, each line shown in Figure 10 lies within a band of uncertainty whose width depends on the standard deviation of the measurements and on the confidence limits chosen. Table V shows the range in which the slope constants can vary for a 95% confidence limit. Also reported in this table are the products of the standardized partial regression coefficients (β) and their corresponding correlation coefficients (r). Each product directly gives the fraction of the loss tangent variance caused by a given impurity ion, and the sum of $r\beta$ over all the impurity species is R^2. Since R^2 is 0.86 at 10^6 c/s, most of the variance of tan δ can evidently be ascribed to the impurities. The residual variance might easily be the result of errors in analyses of the impurity concentrations.

Whereas the slope constants permit the prediction of tan δ for interpolated values of composition, the $r\beta$ products are particularly useful for comparing the relative effects produced by each impurity element. Table V clearly shows the dominant position occupied by Si, which has about seven times the effect of Mg, the second element on the list. Mg has a slightly greater influence than Ti, and Ca, Fe, and Cr have relatively small effects.

It will be shown later in this report that electronic (or hole) conductivity is the primary loss mechanism in alumina at 500°C and 10^5 c/s. Therefore, the powerful influence of Si ions is understandable in the light of their ability to generate shallow traps for both holes and electrons. Holes are trapped at vacant Al^{3+} sites which are formed to compensate the excess positive charge of the Si^{4+}. This concentration of charge also serves to hold electrons in the vicinity of the Si ion sites. Energies deduced from glow curves (Table VI) fix the depth of at least one of these two types of traps at about 1.6 ev.

In contrast to Si^{4+}, Mg^{2+} impurities tend to create oxide ion vacancies. These vacant sites also form shallow traps for electrons, and in addition, the Mg^{2+} sites themselves can trap positive holes. If the charge carriers here are also electrons and/or holes, why do Mg ions have so small an effect as compared to Si? Both are probably about equally soluble in alumina at the concentration levels involved. The most reasonable explanation for this phenomenon is that electrons are more strongly bound to an oxide ion vacancy than to a Si^{4+} ion, and that holes are more deeply entrapped at an Mg^{2+} site than at an Al^{3+} vacancy. This view is supported by glow curve data which yield a trapping energy of about 2.9 ev for either the holes or the electrons.

Titanium ions should be expected to behave like silicon in having a strong influence on tan δ ; nevertheless, the observed effect is actually relatively small. This result cannot be explained by postulating deeper electron and hole traps for Ti since glow curves show that they are actually shallower than those reported for Si. The explanation for the behavior of titanium probably lies in the ready tendency for Ti^{4+} to be reduced to Ti^{3+} in its oxides. Consequently, the influence of surrounding Al^{3+} probably causes the titanium (if it is in a low concentration) to enter the alumina as the trivalent ion, which does not force the creation of cation vacancies. However, fairly shallow electron trapping levels still occur at the titanium sites because of the relative ease with which Ti^{3+} can be oxidized to Ti^{4+}. Consequently, the conductivity is higher than that of pure alumina. These considerations suggest that hole conduction originating from the cation vacancies is an important factor in specimens containing Si.

From charge considerations alone, the behavior of Ca^{2+} might be expected to resemble that of Mg^{2+}. However, the larger radius of the calcium ion probably severely limits its solubility in alumina. Therefore, the actual concentrations of dissolved Ca^{2+} are probably appreciably lower than those given for the compositions of the ceramics.

The low slope constants given by Cr and Fe are not surprising since under oxidizing conditions low concentrations of these impurities almost certainly enter alumina in the trivalent state. Moreover, unlike titanium, Fe^{3+} and Cr^{3+} are not readily further oxidized to tetravalent ions.

Therefore, although localized energy levels are associated with Fe^{3+} and Cr^{3+} sites, they correspond to rather deep traps.

2. 10^2 Cycles Per Second

Loss phenomena at 10^2 c/s and 500°C are more complex than at the higher frequency because ionic as well as electronic mechanisms play an important role. Ions migrating individually may carry charge between the measuring electrodes or, by associating into dipolar groups, they may oscillate in an AC field. Both of these ionic processes are facilitated by the presence of vacancies and to a lesser extent by strain producing foreign ions. These same lattice defects also activate electrons or positive holes which add their contributions to the loss tangent. Additional complexity arises from the fact that divalent impurities tend to create oxide vacancies which mobilize diffusion of anions, whereas tetravalent ions produce cation vacancies which accelerates cation diffusion. However, if both types of impurities are present, they can compensate each other, and the total number of vacancies might be considerably lower than for each type alone. This will tend to reduce the conductivity losses, but association of the divalent and tetravalent cations may form dipoles which will add to the polarization losses.

For the reasons outlined above, departures from the simple linear regression equation might be expected. Actually, a semi logarithmic function:

$$Y_o = b_1 \log x_1 + b_2 \log x_2 + \ldots + \log A \qquad (2)$$

accounts for a greater portion of the variance of tan δ than the linear form. With this refinement, R is about 0.80, and the dominance of Si is clearly evident (Table V). This preeminence of Si at 10^2 c/s as well as at 10^6 c/s is not surprising in view of the fact that the processes which tend to activate electrons are also effective in raising ionic conductivity. Moreover, the electronic conductivity may comprise an appreciable part of the losses at the lower frequency.

C. Effect of Impurities on the Activation Energy of Conduction

The close approximation to linearity of the 500°C curve of k'' vs. frequency (f) indicates that the losses are primarily derived from conductivity effects. Therefore, the activation energy of conduction may be obtained at this temperature by first computing the dielectric conductivity (σ) from k' and tan δ :

$$\sigma = \frac{f\, k' \tan \delta}{1.8 \times 10^{12}} \qquad (3)$$

and plotting log σ against $10^3/T$. Figure 11 shows the resulting curves for pure alumina, and for specimens contaminated with Si (A32), Ti (A45), Mg (A37), Ca (A21), Fe (A57), and Cr (A61). If a single conduction mechanism were operating over the temperature range, the semi log

plot would give a straight line, and the activation energy E would be given by:

$$E = \frac{1.72 \times 10^{-4} \ln \sigma_2/\sigma_1}{1/T_1 - 1/T_2} \quad (4)$$

The curvature of the semi log plots demonstrates the existence of more than one mechanism: probably surface conduction at the lower temperatures and bulk conduction in the upper regions. The activation energies of bulk conduction were calculated by drawing straight lines tangent to the various curves near 500°C. Values of E obtained in this manner are listed in Table VI. The striking similarity of the activation energies indicates the operation of one conduction mechanism for all of the specimens except that containing introduced Mg^{2+}. An explanation of this phenomenon is provided by a comparison of the energies obtained from the conductivity data with trap depths calculated from glow curves. The similarity of the predominant activation energy (1.2 to 1.6 ev) and the estimated trapping energies at Ti and Si sites (1.2 and 1.6 ev respectively) strongly suggests that electrons (or holes) from these traps are the dominant charge carriers. Since A8, A61, and A32 do not contain detectable amounts of Ti, Si appears to be the source of conduction electrons in at least these ceramics. Results given by A57, A21, and A61 are more inconclusive since these compositions contain both Ti and Si. Specimen A37 is unique in having a value of E (2.0 ev) much too high to be related to Si or Ti alone. However, this value is consistent with an average of the trapping energies of Si and Mg.

In summary, activation energy data at 10^5 c/s and 500°C show that the dielectric losses are primarily caused by an extrinsic electronic conduction which stems from Si (and possibly Ti) and to a lesser extent, Mg impurities in the alumina structure. These results provide independent corroboration of the conclusions derived from the multiple regression analysis.

D. Polarization Effects

1. Dispersion of the Dielectric Constant

With increasing temperature k' at 10^2 c/s begins to rise at a faster rate than it does at higher frequencies (Figure 9). This leads to a dispersion of k' which increases up to 500°C. Examination of Table IV shows that with the exception of specimens containing appreciable Mg, the dispersion is fairly proportional to tan δ at 10^6 c/s and 500°C - and therefore to the electronic conductivity of the bulk ceramic. This spread of k' can probably be attributed to the occurrence of highly resistive barrier layers at one or both of the measuring electrodes. Together with the bulk ceramic, such layers form a variant of the Maxwell-Wagner two layer condenser (Ref. 9). If such a condition exists, calcu-

lations of k' based on the assumption of a single homogeneous dielectric are in error, giving k' values that are anomalously high.

Cohen (Ref. 4) has suggested that the barrier layers at the measuring electrodes may be created by either electronic or electrolytic processes. The electronic mechanism is based on the known development of a barrier potential at a rectifier contact. In the present case there are two opposed rectifier contacts in which the alumina is the semi conductor. The electrolytic process is similar to the polarization of a cell; positive or negative ions accumulate at one or both of the electrodes. The electrolytic phenomenon may serve to explain the unusually high dispersion of k' displayed by specimens containing high levels of Mg. Because of its lower charge, Mg^{2+} should be more mobile than Si^{4+}, Ti^{4+}, Cr^{3+}, or Fe^{3+}, and, as a result of its smaller radius, it should also have a higher mobility than Ca^{2+}. Consequently, although the electrolytic polarization effect may augment the rectifier barrier potential to some extent for all of the ceramics, the ionic contribution should be a maximum for magnesia doped specimens.

2. Intragranular Polarization

Peaks occurring in the k'' vs. frequency curves of Figures 1, 2, 5 and possibly 6 and 8, may be caused by either an ionic relaxation process or an interfacial polarization governed by high resistance layers at the grain boundaries. The fact that these peaks do not appear in the higher temperature curves is consistent with both processes: rising temperature should on the one hand increasingly dissociate the dipolar ionic complexes, and on the other it should raise electronic energies to a point where they easily traverse the grain boundary barriers. The question of which of the two processes is primarily responsible for the polarization peaks might, however, be resolved by considering the effects produced by the various impurity ions. Examination of Figures 1 to 8 shows that the maxima appear mainly in the curves of the "pure" aluminas or in those containing impurities which have a relatively small effect on $\tan\delta$. In contrast, Si^{4+} effectively removes the peak in the temperature range studied. These results support the interfacial polarization hypothesis for the following reasons:

a. Introduction of Si^{4+} ions into alumina creates cation vacancies which should produce an increase in the number of dipolar ionic groups. However, the observed effect of Si is actually to lower the polarization.

b. Because of its very pronounced amplification of the bulk electronic conductivity, it would not be surprising if Si^{4+} produced a similar effect at the grain boundaries. As a result, electrons are freer to move from grain to grain at a given temperature and the interfacial polarization should be reduced - as is actually observed.

c. As a converse to a. and b., "pure" ceramics should provide a minimum opportunity for the creation of ionic dipoles and optimum conditions for resistive grain surface barriers. Since the polarization is

particularly evident in this case (Figure 1), the electronic hypothesis is confirmed.

If, as the evidence suggests, the electronic process is indeed the cause of the polarization, the relaxation times corresponding to the peak frequencies give an estimate of the average drift velocity of the carriers under the measuring potential. During the course of one complete cycle, the carriers travel a distance equal to twice the grain diameter. At a peak frequency of approximately 10^5 c/s (Figure 1) and a grain diameter of 0.003 cms for "pure" alumina, the drift velocity is about 600 cm/sec. Since the measuring potential across a specimen one-half cm thick was 20 volts, the carrier mobility at 25°C is $\frac{600 \text{ cm/sec}}{40 \text{ volts/cm}}$ or 15 cm^2/volt sec. Figure 5 shows a shift of the peak frequency to about 2 x 10^3 c/s, which cannot be entirely attributed to the larger grain size of the iron doped specimen. This shift may be due to a change in measuring potential from 20 to 2 volts/.5 cm; according to W. B. Westphal (Ref. 10) measurements on lossy specimens were carried out at the lower potential. Assuming 4 volts/cm to be correct, the mobility, based on a grain size of 0.011 cms, is 11 cm^2/volt sec. This value agrees surprisingly well with 15 cm^2/volt sec calculated for "pure" alumina.

Although no other carrier mobility data was found for alumina, several values are listed for MgO, a similarly insulating ionic oxide. These values include 2 cm^2/volt sec at room temperature (from measurements of the photo induced Hall effect by Yamaka and Sawamoto (Ref. 11), and 27, 50, and 71 cm^2 volt/sec at 60°C (calculated for different ratios of optical to acoustical mode scattering by Hutson (Ref. 12) from the measurements of Marshall, Pomerantz and Shatas (Ref. 13).

E. The Dielectric Constant

Aside from the dispersion effects previously attributed to the existence of high resistance electrode barrier layers, there occurs a nearly linear positive variation of k' with temperature of about 112 ppm/°C. This rise appears to be characteristic of alumina itself: variations in the impurity composition of the specimens had practically no influence on the temperature coefficient. Since a major objective of the present program was the control of the variation of k' it appeared that attention had to be given to an approach other than purification or the introduction of low concentrations of various impurities. A reasonable plan was the preparation of a two phase ceramic in which the major compound would be alumina and the accessory would be a phase having a negative temperature coefficient of k'. Such materials are found in the titanate groups; e.g., TiO_2, $CaTiO_3$, and $SrTiO_3$. The first of these cannot be used because, upon firing with alumina, it reacts to form aluminum titanate - which does not have the required electrical characteristics. Fortunately, preliminary experiments showed that $CaTiO_3$ does not react with alumina to any great degree and most of

the compound remains as a separate phase. $SrTiO_3$ may be expected to behave in a similar manner.

Since k' vs. T curves are available for $CaTiO_3$ and $SrTiO_3$ at temperatures up to 500°C (Ref. 14) the compositions required to achieve a final curve of any desired slope may be estimated by differentiating Lichteneckers logarithmic mixing rule (Ref. 15) with respect to temperature. If it is desired that the mixture have an invariant dielectric constant, the resulting equation is:

$$C_A = \frac{\frac{100}{k'_B}\frac{d\,k'_B}{dT}}{\frac{1}{k'_B}\frac{d\,k'_B}{dT} - \frac{1}{k'_A}\frac{d\,k'_A}{dT}} \qquad (5)$$

where k'_A and k'_B are respectively the dielectric constants at 25°C of the titanate and the alumina, and C_A is the concentration in vol % of the titanate.

For the purposes of a rough estimate, an average slope may be assumed for the k' vs. T curves of the titanates despite the fact that these curves depart appreciably from linearity. With this assumption, the required concentrations of $CaTiO_3$ and $SrTiO_3$ are respectively 13% and 10% for a dielectric having a minimum temperature variation of k'. Actually, since the linearity assumption is crude, a mixture will show the most complete negative compensation at low temperatures.

Unfortunately, introduction of a titanate phase into an alumina ceramic is bound to raise its loss tangent as well as compensate the rise of k'. Therefore it would be desirable to minimize the titanate concentration by using a compound having the highest possible negative temperature coefficient of k'. This might be a solid solution of Ba and Sr titanates having a Curie temperature just below the lowest use temperature of the dielectric. However, such materials also tend to have more curvilinear functions of k' vs. T, which would prevent good compensation of the alumina over a wide temperature range. This problem of balancing titanate concentration against wide range compensation will be considered during the future course of the program.

Dielectric losses of self compensating ceramics might be reduced by insuring complete oxidation of the Ti ions in the titanate phase. Such an oxidized condition might be obtained by annealing the fired ceramic in oxygen or by incorporating a slight excess of divalent cations (Mg, Ca, or Sr) beyond the stoichiometric ratio $MO:TiO_2$. The second procedure produces a deficiency of positive charge which drives the titanium to the +4 state as a counterbalancing measure.

Exploratory experiments on self compensating ceramics were carried out with batches containing 5 and 10 weight percent of TAM com-

mercial calcium titanate and ALUCER MA aluminum oxide (Gulton Industries, Inc.). Of these two compositions, the 10% $CaTiO_3$ discs had a dielectric constant of about 11.4-11.7, which at 10^7 c/s, remained essentially constant to 250°C.

At higher temperatures k' rose sharply - reflecting the influence of electrode barrier layers. In the microwave region this effect should be reduced, and the invariancy of k' should extend to higher temperatures. As might be expected, the loss tangents (at 10^7 c/s and 500°C) of 10% $CaTiO_3$-90% Al_2O_3 specimens were high (0.04-0.05) compared to that of "pure" alumina (about 0.0002). Nevertheless, they compare quite favorably with the value of 0.1 reported by MIT (Ref. 16) for Pyroceram 9606.

V. SUMMARY AND FUTURE WORK

Despite an inability to fabricate high purity alumina into ceramics with densities higher than about 3.67 g/cm^3, measurements of tan δ and k' have clearly demonstrated the relative effects of the common impurity ions. A multiple regression analysis of electrical data provided by doped specimens has shown that in order of diminishing influence, impurities may be grouped as follows: Si, Mg, Ti, Ca, Cr, and Fe. The dominance of Si and the secondary but still respectable effect of Mg was corroborated by activation energies of conduction calculated at 500°C and 10^5 c/s. Energies determined for "pure" and doped specimens (except in the case of Mg) agreed well with the depths of traps associated with Si impurities as derived from glow curves. Specimens containing a low concentration of added Mg had activation energies intermediate between the depths of the traps produced by Mg and Si.

Replotting the measured loss tangents as k'' vs. frequency curves revealed a series of small polarization peaks which were most pronounced for "pure" alumina specimens, and for discs doped with Fe. These peaks are interpreted to mark the relaxation times of an interfacial polarization controlled by grain boundaries. Applying this hypothesis to known information on the grain size of the ceramics, the potential difference used in the electrical measurements, and the thickness of the specimen discs, leads to an estimated carrier mobility of 11 to 15 cm^2/volt sec for alumina at 25°C.

Increasing the purity of aluminum oxide ceramics is not sufficient to remove a fairly constant rise of k' with T of slightly over 100 ppm/°C. Reduction of this temperature variation is being approached from the view point of preparing a two phase ceramic in which a titanate compound serves to compensate the alumina. Preliminary results have shown that a composition containing 10% $CaTiO_3$ and 90% alumina has an invariant k' up to about 250°C at 10^7 c/s, and the losses at 500°C and 10^7 c/s are somewhat lower than those of Pyroceram 9606.

This report has introduced two major problems whose investigation will comprise a major part of the program's third year. The densification of high purity alumina to a low porosity ceramic will be attempted by hot pressing high surface alumina in an argon atmosphere, and through the use of such non-contaminating additives as aluminum metal. Two phase alumina ceramics will be studied with the aim of reducing the losses that are created by introduction of a titanate compound. Reduction of the total titanium concentration through the use of $SrTiO_3$-$BaTiO_3$ solid solutions as the compensating phase, and oxidation of the titanium ions by oxygen annealing and adjustment of the M^{2+} Ti^{4+} ratio will both be investigated.

In addition to these two problems, attention will also be given to the mechanical properties of "pure" dense alumina and of titanate-bearing alumina ceramics at temperatures up to about 1000°C. Finally, thermoelectric power and photo induced Hall effect measurements will be used to provide additional information on the types and mobilities of the charge carriers in "pure" alumina and in the doped ceramic discs previously used for measurements of tan δ and k'.

Table I

ANALYSES OF ALUMINA CERAMICS USED FOR ELECTRICAL EVALUATION

No.	Firing Temp. °C	Bulk Density gm/cm^3	Concentration ppm									
			Si	Ti	Fe	Cr	Mg	Ca	Ni	Cu	Co	Ag
batch	-	-	20	-	10	4	30	10	5	2	-	-
A8	1870*	3.67	20	-	18	4	22	11	8	-	-	-
A13	1900*	3.43	35	-	15	1	17	20	15	4	-	-
A7	1840*	3.41	60	-	60	4	30	15	5	3	-	-
A32	1900	3.41	110	-	6	-	5	2	-	-	-	-
A23	1900	3.41	320	70	75	-	65	25	4	-	4	5
A24	1900	3.41	1050	75	140	-	55	15	5	2	4	9
A58	1920	3.63	600	-	11	-	470	4	-	-	-	-
A37	1920	3.65	12	20	18	2	480	70	-	-	-	-
A59	1920	3.65	19	-	12	-	1200	4	-	-	-	-
A38	1920	3.39	15	35	16	3	20	60	-	-	-	1
A21	1915	3.39	35	30	8	-	40	320	5	-	6	8
A39	1920		37	18	17	4	8	600	-	-	-	1
A22	1915	3.37	60	50	7	-	50	800	-	-	4	9
A14	1905*	3.45	40	-	12	-	12	800	8	8	-	-
A56	1920	3.43	25	-	70	4	20	9	-	-	-	-

Table I (cont'd.)

ANALYSES OF ALUMINA CERAMICS USED FOR ELECTRICAL EVALUATION

No.	Firing Temp. °C	Bulk Density gm/cm^3	Concentration ppm									
			Si	Ti	Fe	Cr	Mg	Ca	Ni	Cu	Co	Ag
A25	1920	3.29	50	80	350	-	60	10	5	1	5	7
A57	1920	3.47	20	9	670	3	16	8	-	-	-	-
A26	1920	3.37	30	20	750	-	25	6	-	-	4	7
A60	1920	3.39	19	-	12	68	21	6	-	-	-	-
A61	1920	3.47	10	-	25	680	18	6	-	-	-	-
A45	1915	3.31	36	60	28	3	34	22	-	-	-	2
A30	1920	3.43	40	600	55	-	30	10	4	5	1	6
A63	1920	3.65	14	950	85	1	24	1470	-	1	-	1

*All of the tabulated specimens except A7, A8, A13, and A14 were fired in a gas-oxygen furnace under oxidizing conditions. A7 and A8 were fired in stagnant air in an inductively heated furnace. These specimens were probably exposed to a fairly high concentration of CO which formed at the graphite susceptor and leaked into the combustion tube through cracks. A13 and A14 were also fired in the inductively heated furnace but in a stream of flowing air.

Table II

EFFECT OF CALCINING TEMPERATURE ON THE PROPERTIES OF ALUMINA BATCH AND CERAMICS

Max. Temp. at which Precipitated Hydrate was Calcined (°C)	Surface Area of Calcined Powder (meters^2/gm)[1]	Mean Particle Size (microns)[2]	Green Density of Disc Pressed at 15,000 psi (gm/cm^3)	Density of Discs Fired at 1905°C (gm/cm^3)
1000	75.6	1.6	1.43	3.22
1100	51.3	1.2	1.58	3.35
1300	5.7	1.6	2.01	3.38

[1] By nitrogen absorption

[2] By Fisher subsieve analyzer

Table III

PARTICLE SIZE OF ALUMINA CERAMICS

No.	Predominant Size (microns)	Size Range (microns)	Bulk Density (gm/cm^3)
A13	30	20- 40	3.43
A32 (Si)	-	30- 80	3.41
A56 (Fe)	110	20-110	3.43
A37 (Mg)	15-20	15- 55	3.65
A45 (Ti)	15-20	15- 55	3.31

Table IV

LOSS TANGENTS AND DIELECTRIC CONSTANTS AT 10^2 AND 10^6 CYCLES PER SECOND AND 500° C*

Composition No.	Tan δ 10^2 c/s	k'_1 10^2 c/s	Tan δ 10^6 c/s	k'_2 10^6 c/s	$k'_1 - k'_2$
A8	0.27	10.3	0.0008	9.4	0.9
A7	0.65	11.0	0.0014	8.7	2.3
A32 (Si)	0.90	16.2	0.0032	8.4	7.8
A23 (Si)	6.5	22.6	0.012	8.6	14.0
A24 (Si)	4.3	24.0	0.021	8.6	15.4
A38 (Ca)	0.18	9.0	0.00056	8.4	0.6
A21 (Ca)	1.3	14.2	0.0015	8.5	5.7
A39 (Ca)	0.48	11.1	0.0065	8.7	2.4
A14 (Ca)	1.5	9.8	0.0014	8.6	1.2
A22 (Ca)	3.6	17.0	0.0039	8.3	8.7
A63 (Ca, Ti)	1.3	26.0	0.016	9.2	16.8
A37 (Mg)	3.0	19.2	0.0029	9.6	9.6
A59 (Mg)	2.3	75.0	0.009	9.4	65.6
A58 (Mg, Si)	6.4	40.0	0.026	9.2	30.8
A56 (Fe)	0.8	11.1	0.0022	8.5	2.6
A25 (Fe)	0.7	11.1	0.0012	8.2	2.9
A57 (Fe)	1.0	10.7	0.0023	8.8	1.9
A26 (Fe)	2.7	10.3	0.0021	8.3	2.0
A60 (Cr)	1.2	13.0	0.0021	8.4	4.6
A61 (Cr)	2.0	12.2	0.0017	8.6	3.6
A45 (Ti)	1.1	15.5	0.0056	8.2	7.3
A30 (Ti)	1.6	19.2	0.0062	8.6	10.6

* Taken from measurements carried out at the Laboratory for Insulation Research of MIT.

Table V

EFFECT OF IMPURITY CONCENTRATION (X)
ON THE LOSS TANGENT (Y) OF ALUMINA CERAMICS

Impurity Ion	10^6 c/s and 500°C $Y_o = b_1X_1 + b_2X_2 \ldots + A$ (A = approx. 0.001)			10^2 c/s and 500°C (1) $Y_o = b_1 \log X_1 + b_2 \log X_2 \ldots + \log A$		
	Slope Constant b	Fiducial Limits of b at 95% Confidence Level	$r\beta$ (2)	Fiducial Limits of $r\beta$ at 95% Confidence Level	$r\beta$ (2)	Fiducial Limits of $r\beta$ at 95% Confidence Level
Si	0.25	± 0.06	0.66	± 0.15	0.40	± 0.22
Mg	0.08	0.02	0.09	0.02	0.23	± 0.18
Ti	0.07	0.02	0.07	0.02	0.00	+ 0.04
Ca	0.03	0.01	0.03	0.01	0.00	+ 0.02
Fe	- 0.02	0.12	0.01	0.06	0.00	+ 0.00
Cr (3)	0.0	-	-	-	-	-

(1) At 10^2 c/s and 500°C, the correlation coefficient for the semi logarithmic relationship was higher than for the simple linear equation.

(2) The term $r\beta$ is the product of the individual correlation coefficient for a given impurity and the standardized partial regression coefficient. It is a direct measure of the proportion of the total variance of tan δ caused by each impurity. The sum of the $r\beta$ terms is the square of the multiple correlation coefficient.

(3) The slope constant of Cr was determined by subtracting the effects of the other ions from samples A60 and A61 and plotting the residual tan δ against the concentration of Cr.

Table VI

ACTIVATION ENERGIES OF CONDUCTION AND TRAPPING ENERGIES OF "PURE" AND DOPED ALUMINA CERAMICS

Introduced Impurity	Activation Energy of Conduction (ev)	Trapping Energy from Glow Curves* (ev)
None	1.2 (A8 annealed in H_2)	-
None	1.3 (A8 annealed in O_2)	-
Si	1.3 (A32)	1.6? *
Ti	1.3 (A45)	1.2? *
Ca	1.6 (A21)	2.5? *
Mg	2.0 (A37)	2.9
Fe	1.3 (A57)	2.4
Cr	1.5 (A61)	-

* Data taken from Atlas and Firestone (Ref. 3)

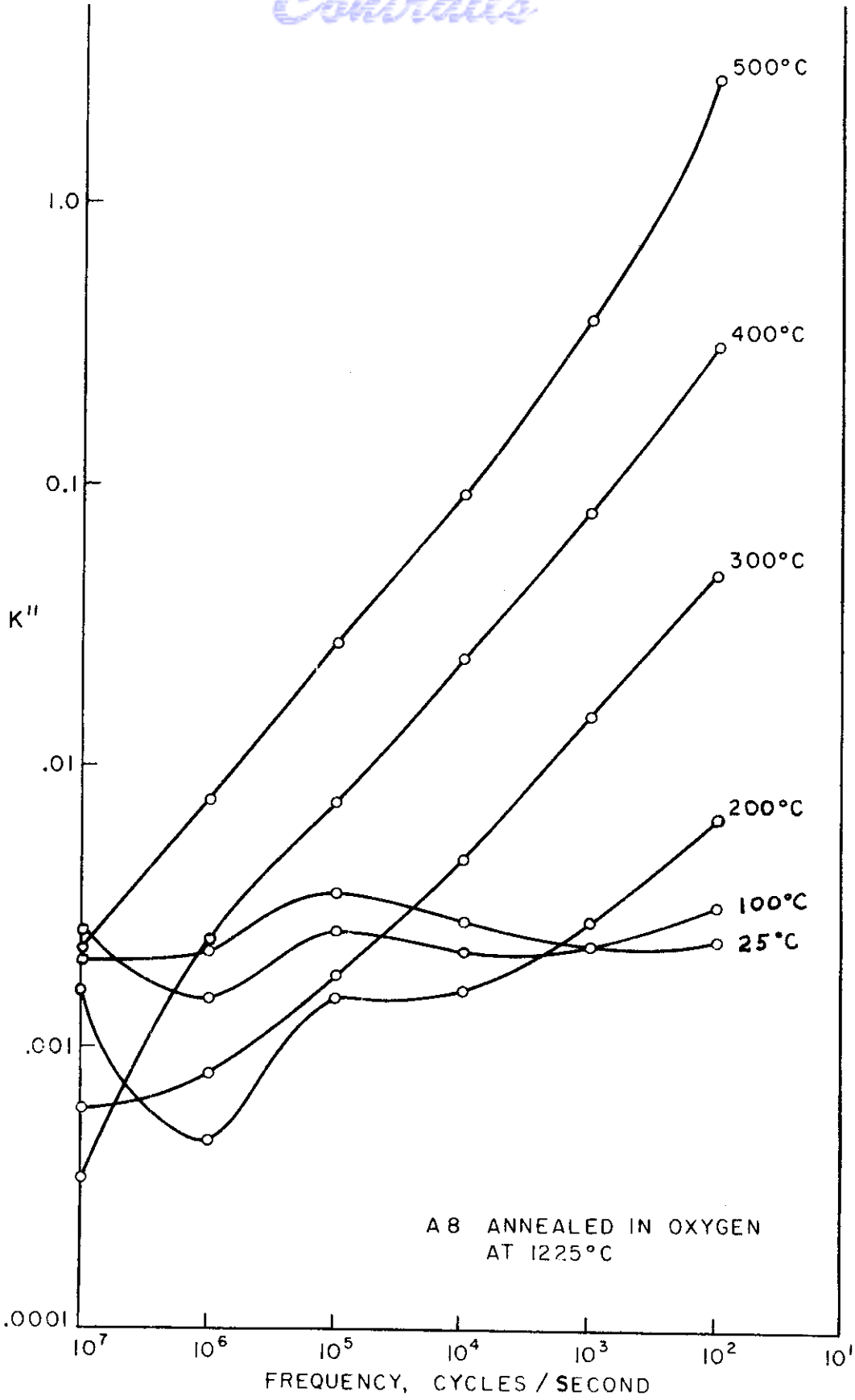

Fig. 1 Frequency Variation of K'' of "Pure" Oxygen Annealed Alumina

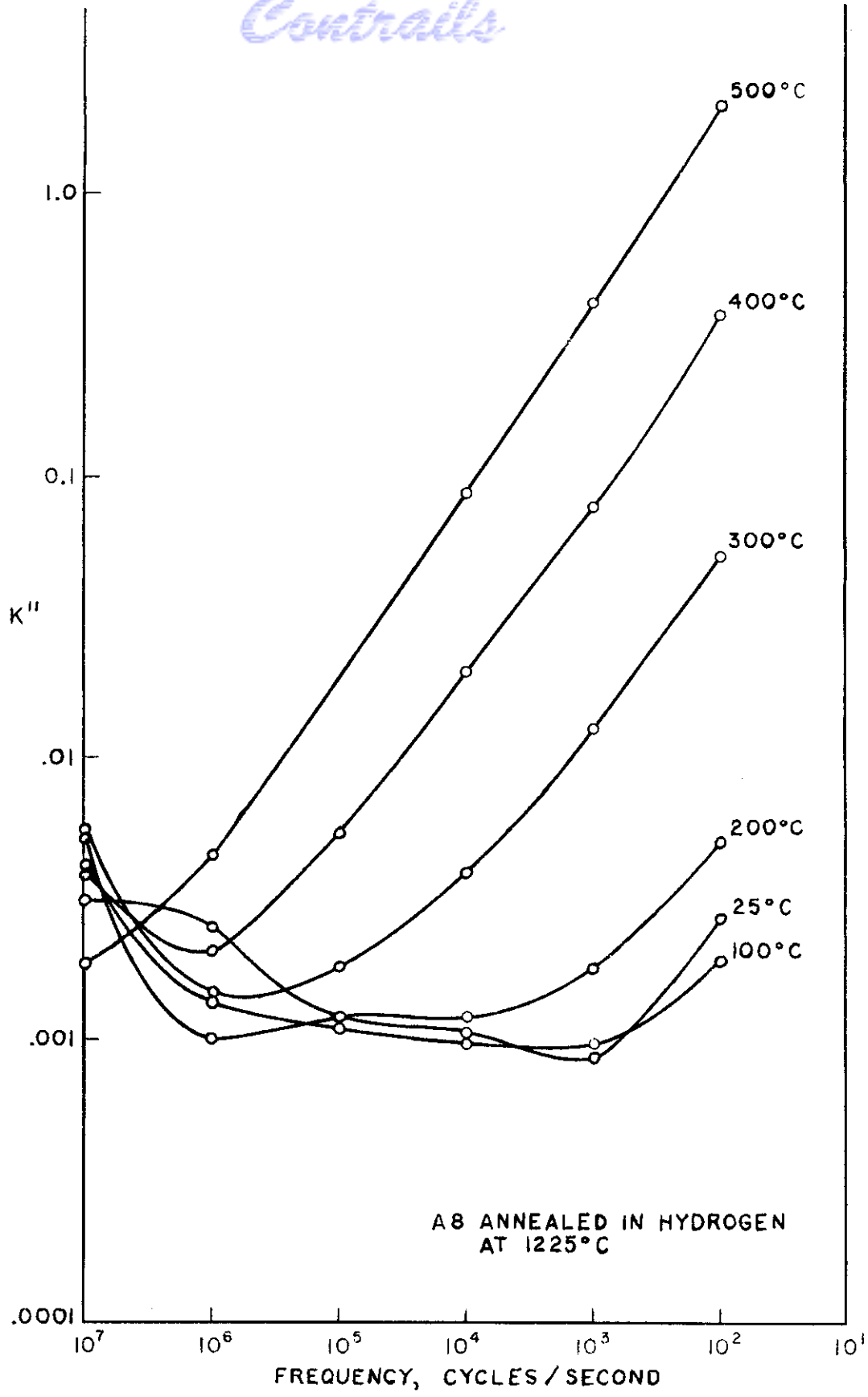

Fig. 2 Frequency Variation of K'' of "Pure" Hydrogen Annealed Alumina

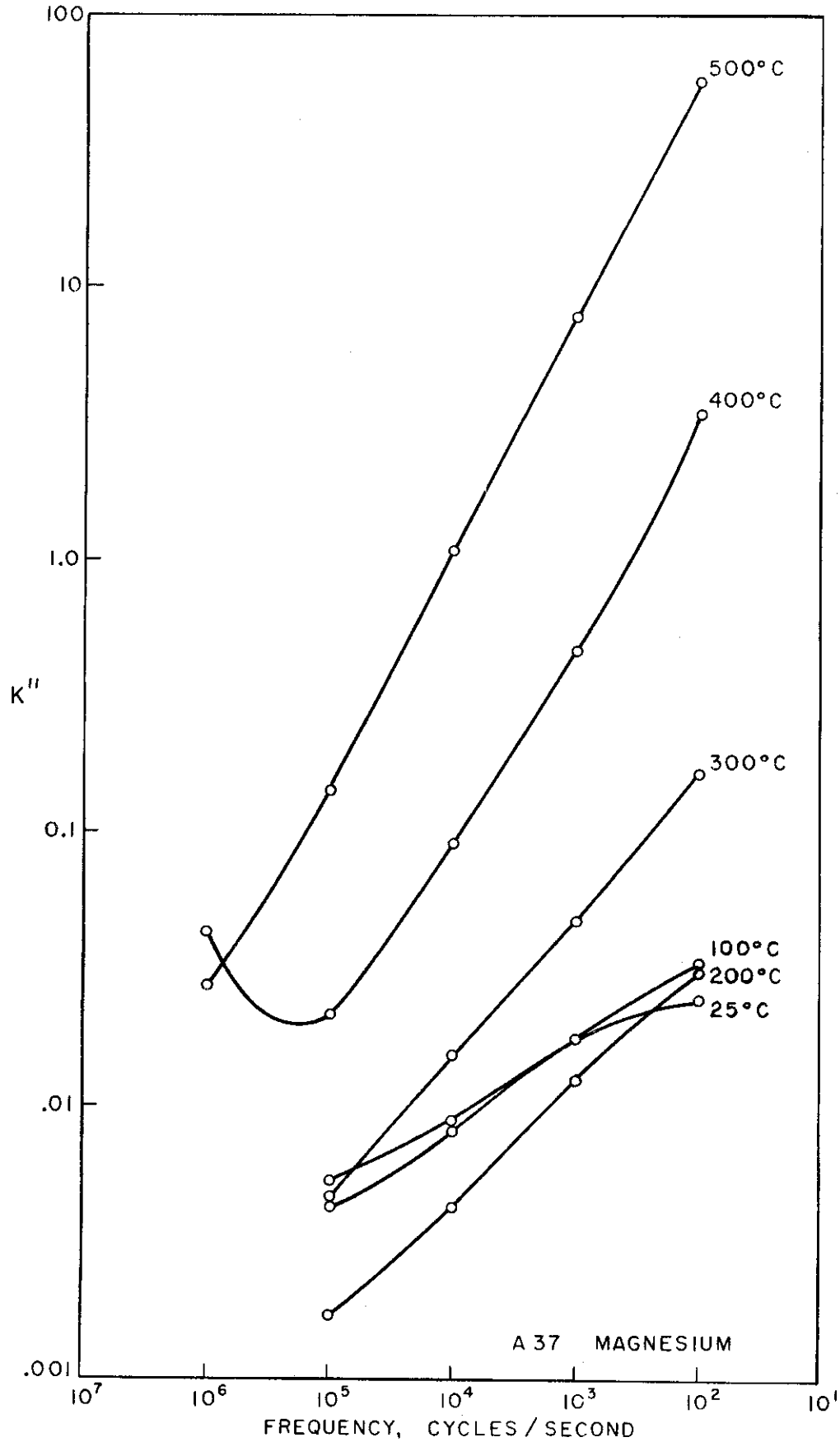

Fig. 3 Frequency Variation of K'' of Alumina Doped with 135 ppm of Mg Ions

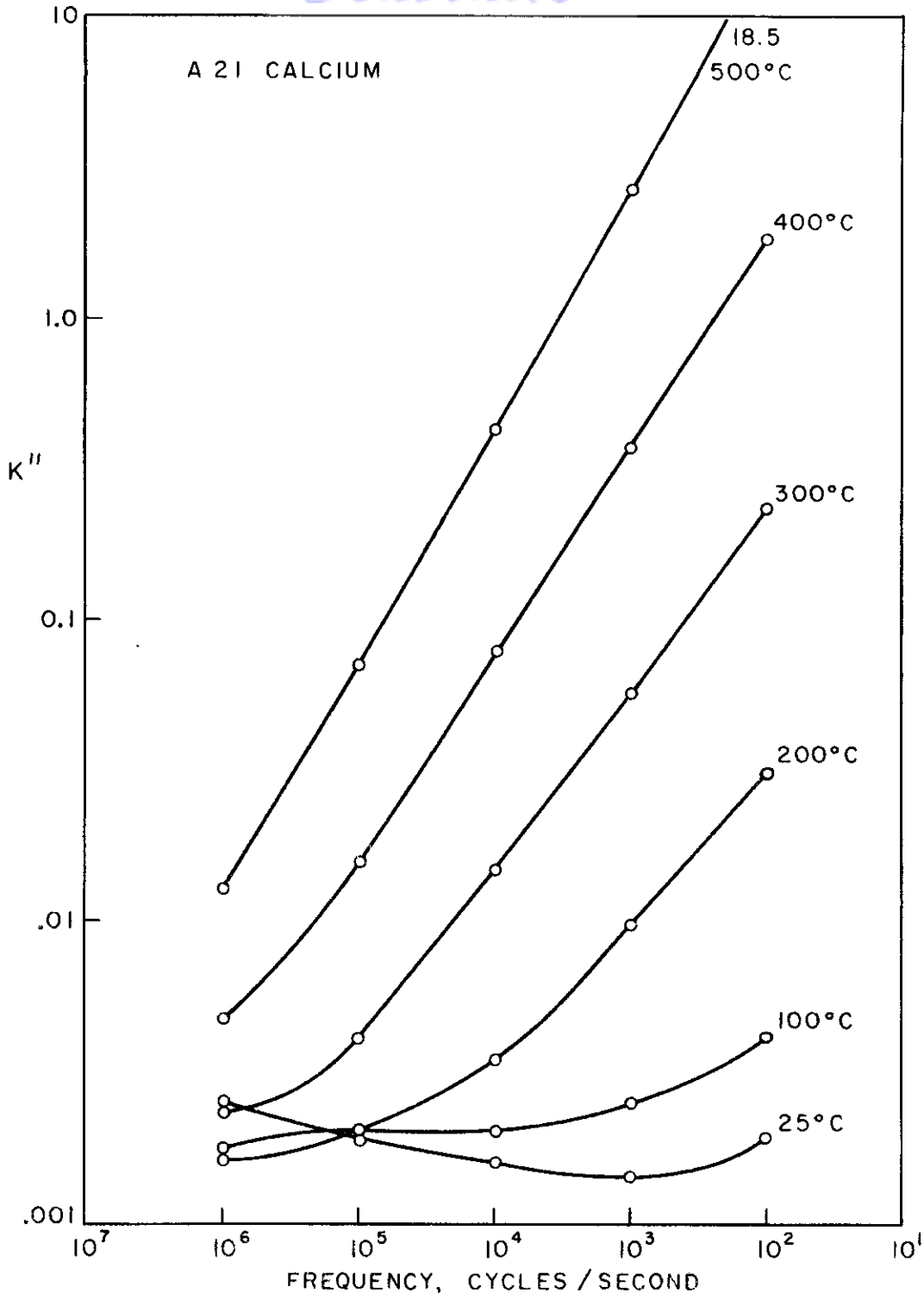

Fig. 4 Frequency Variation of K'' of Alumina Doped with 140 ppm of Ca Ions

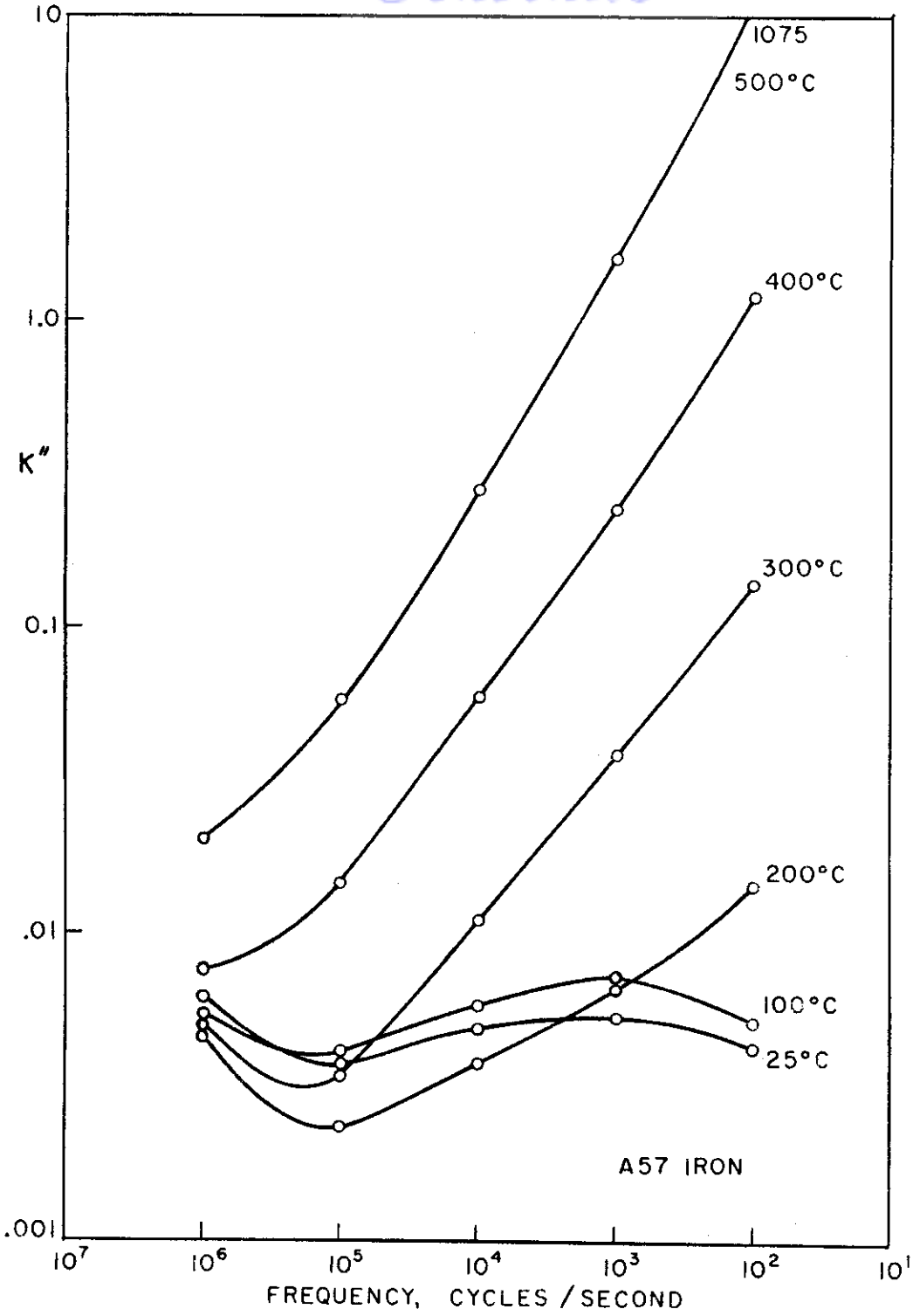

Fig. 5 Frequency Variation of K'' of Alumina Doped with 670 ppm of Fe Ions

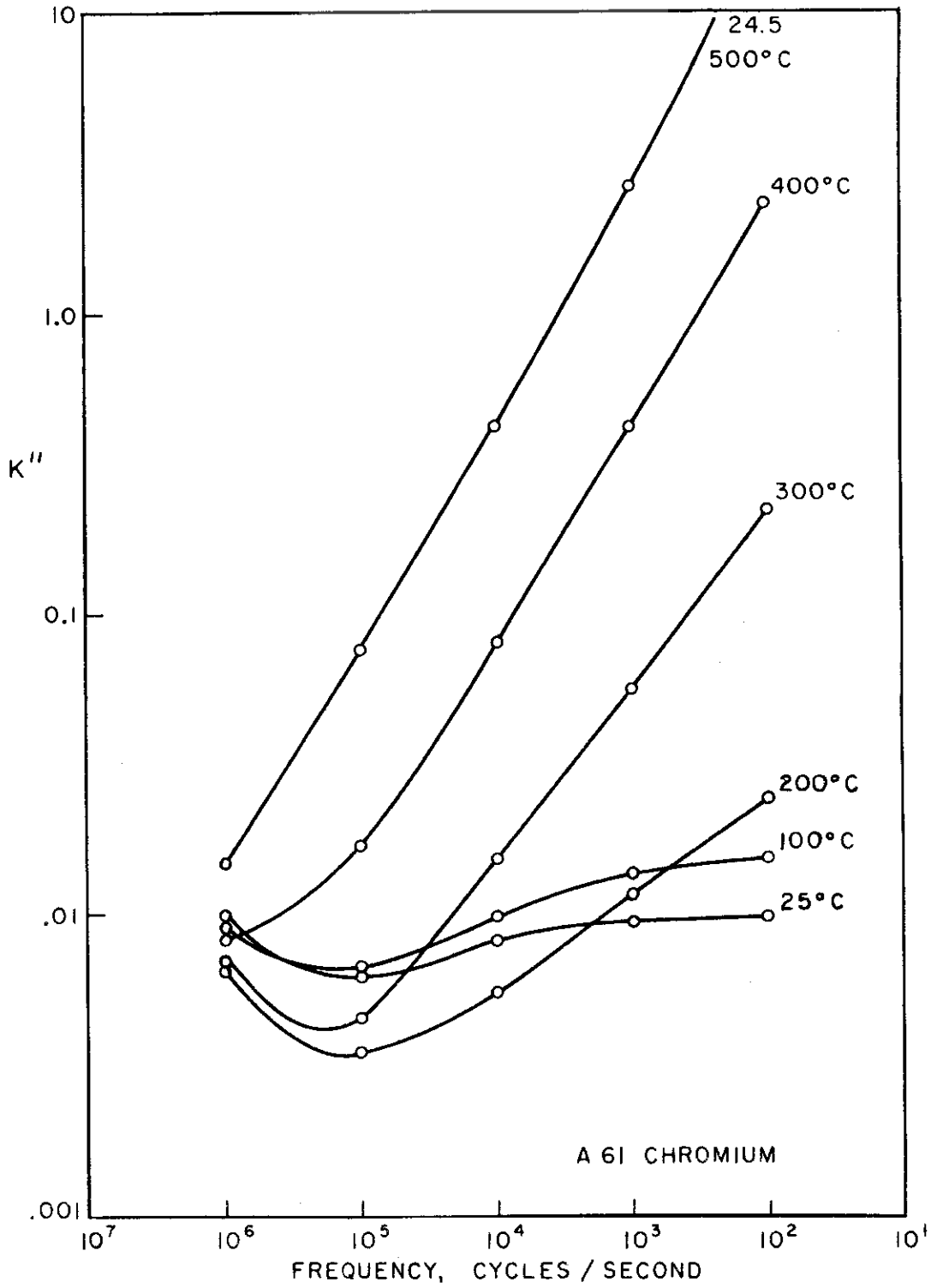

Fig. 6 Frequency Variation of K'' of Alumina Doped with 680 ppm of Cr Ions

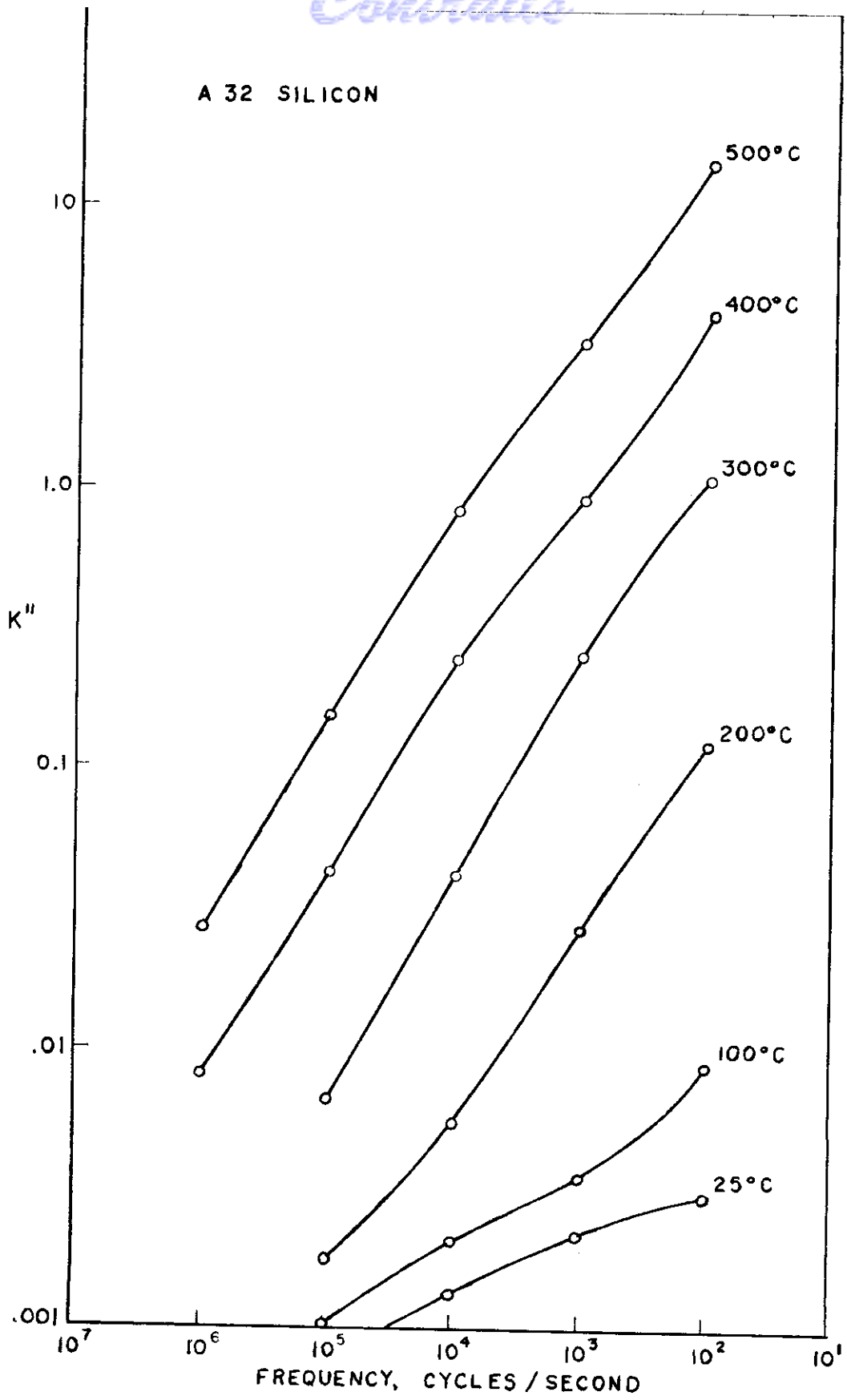

Fig. 7 Frequency Variation of K'' of Alumina Doped with 110 ppm of Si Ions

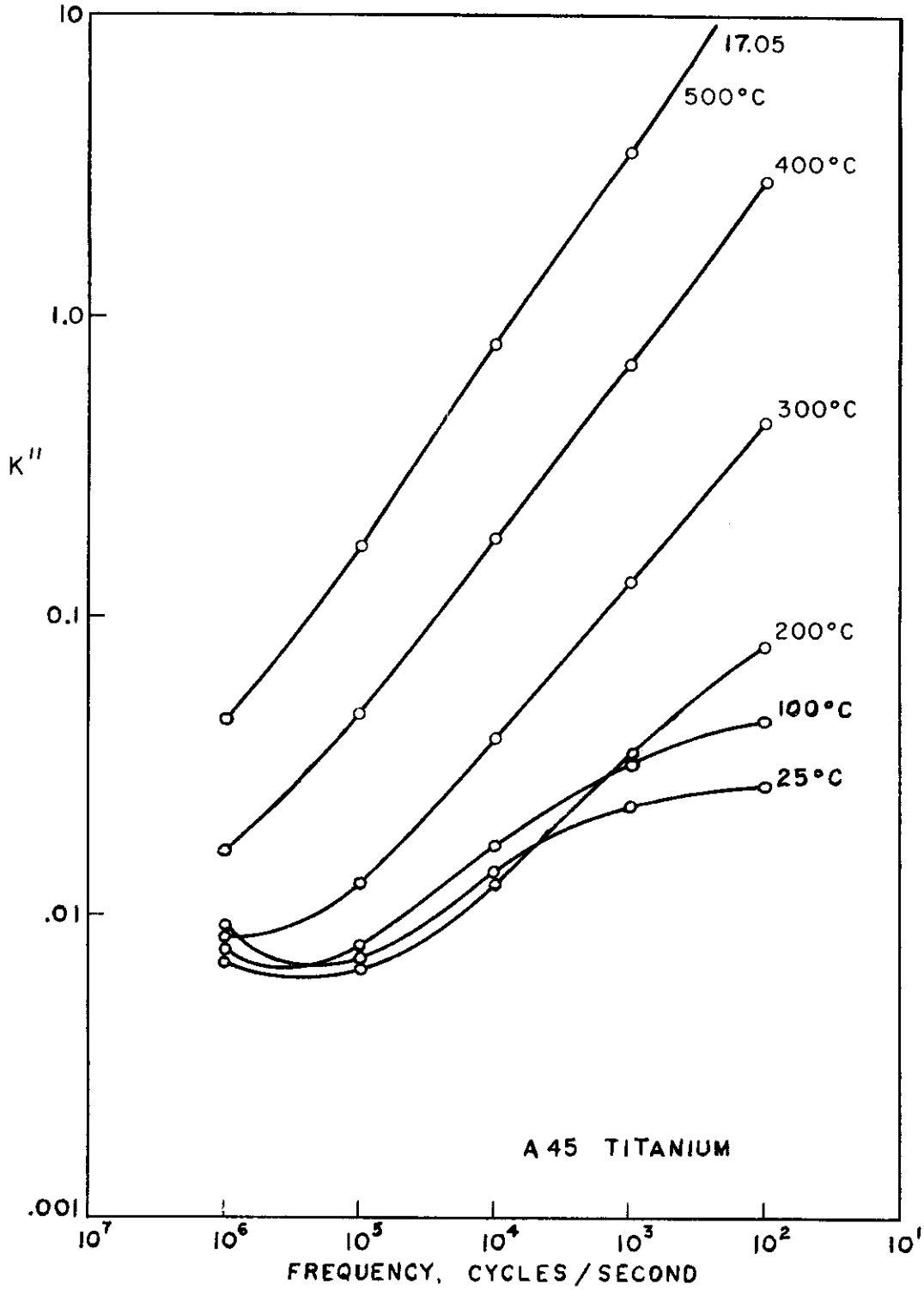

Fig. 8 Frequency Variation of K'' of Alumina Doped with 60 ppm of Ti Ions

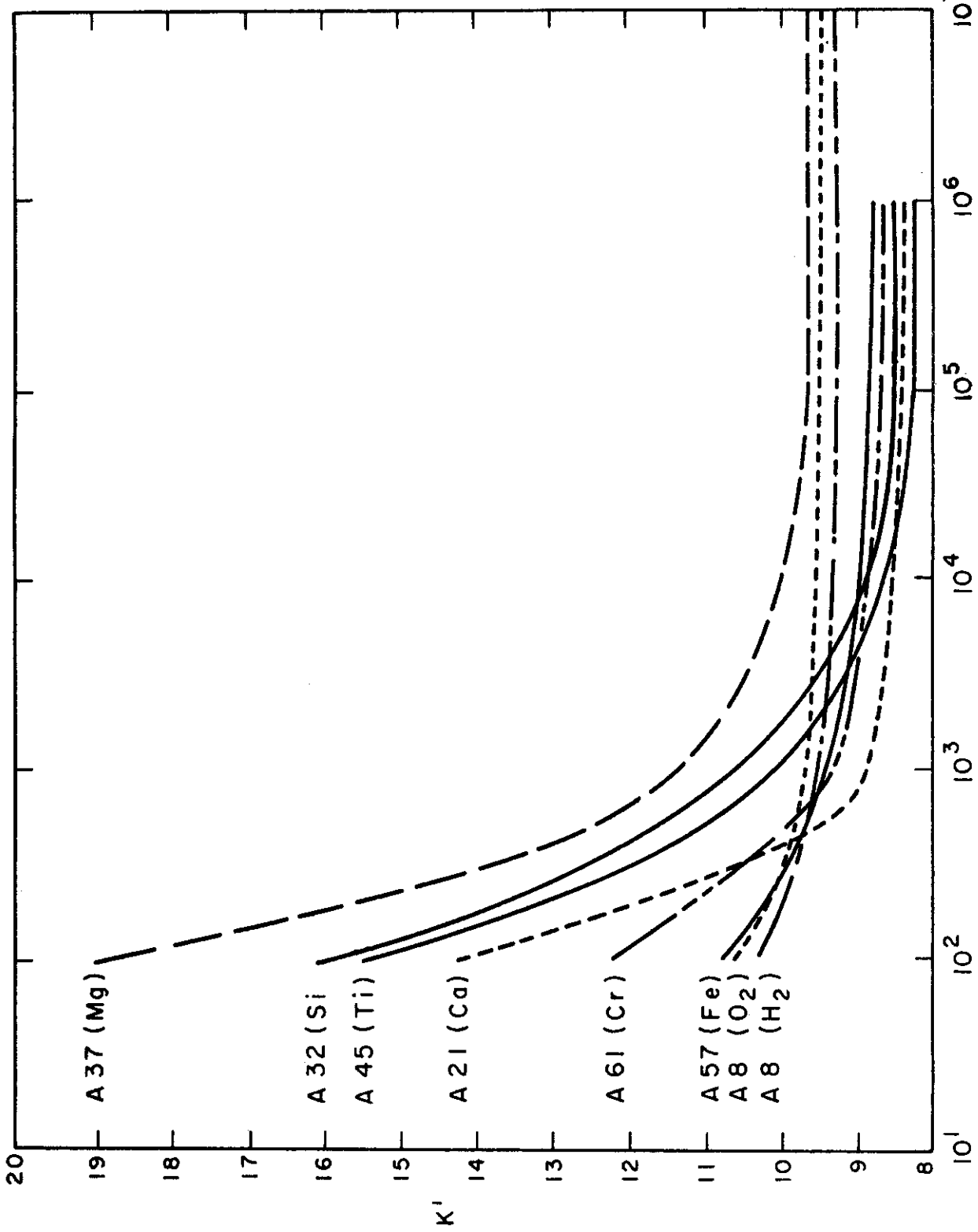

FIG. 9 DIELECTRIC CONSTANT AT 500°C FOR PURE AND DOPED ALUMINAS.

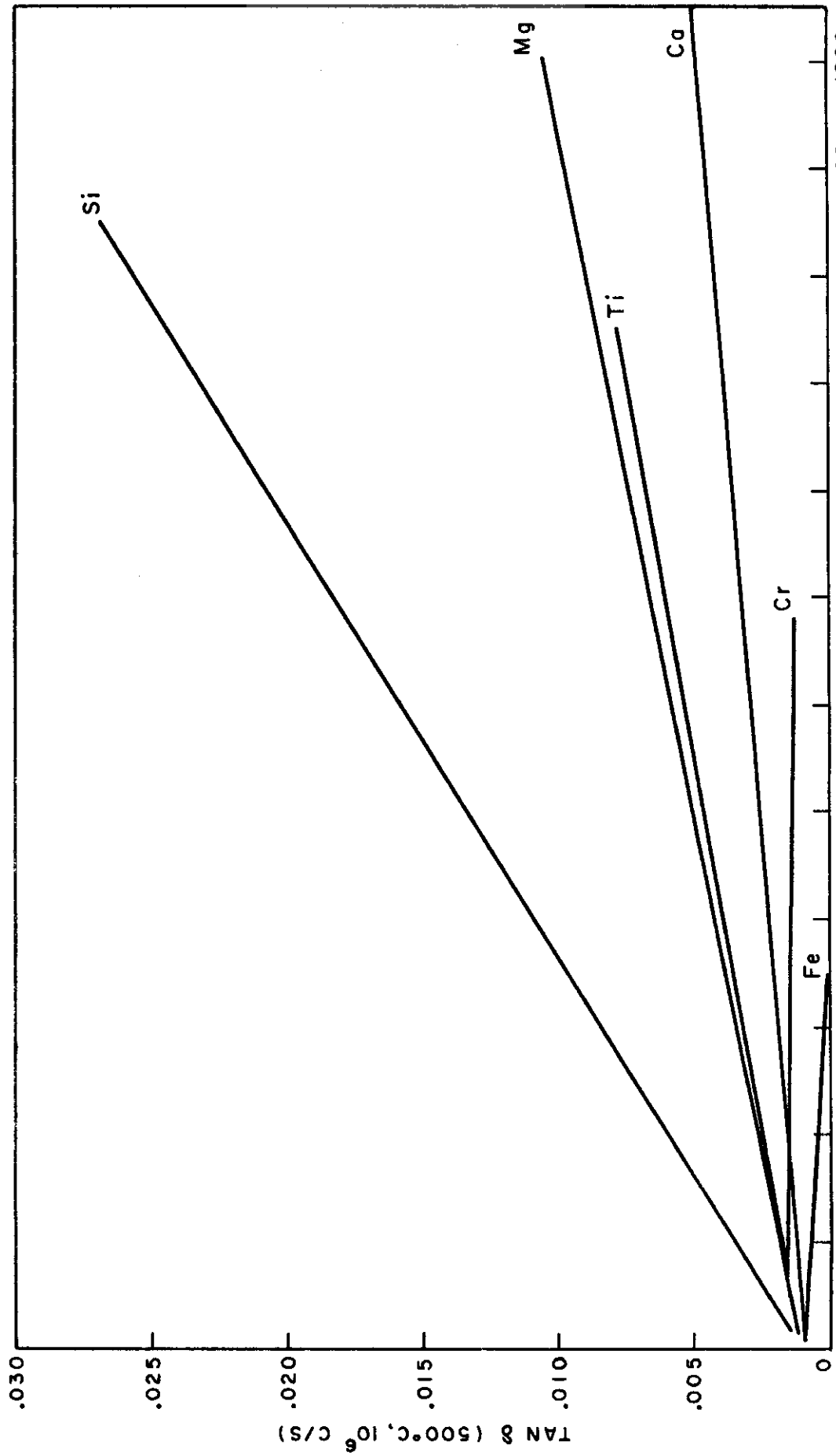

FIG. 10 INFLUENCE OF VARIOUS IMPURITY IONS ON TAN δ (500°C, 10^6 C/S)

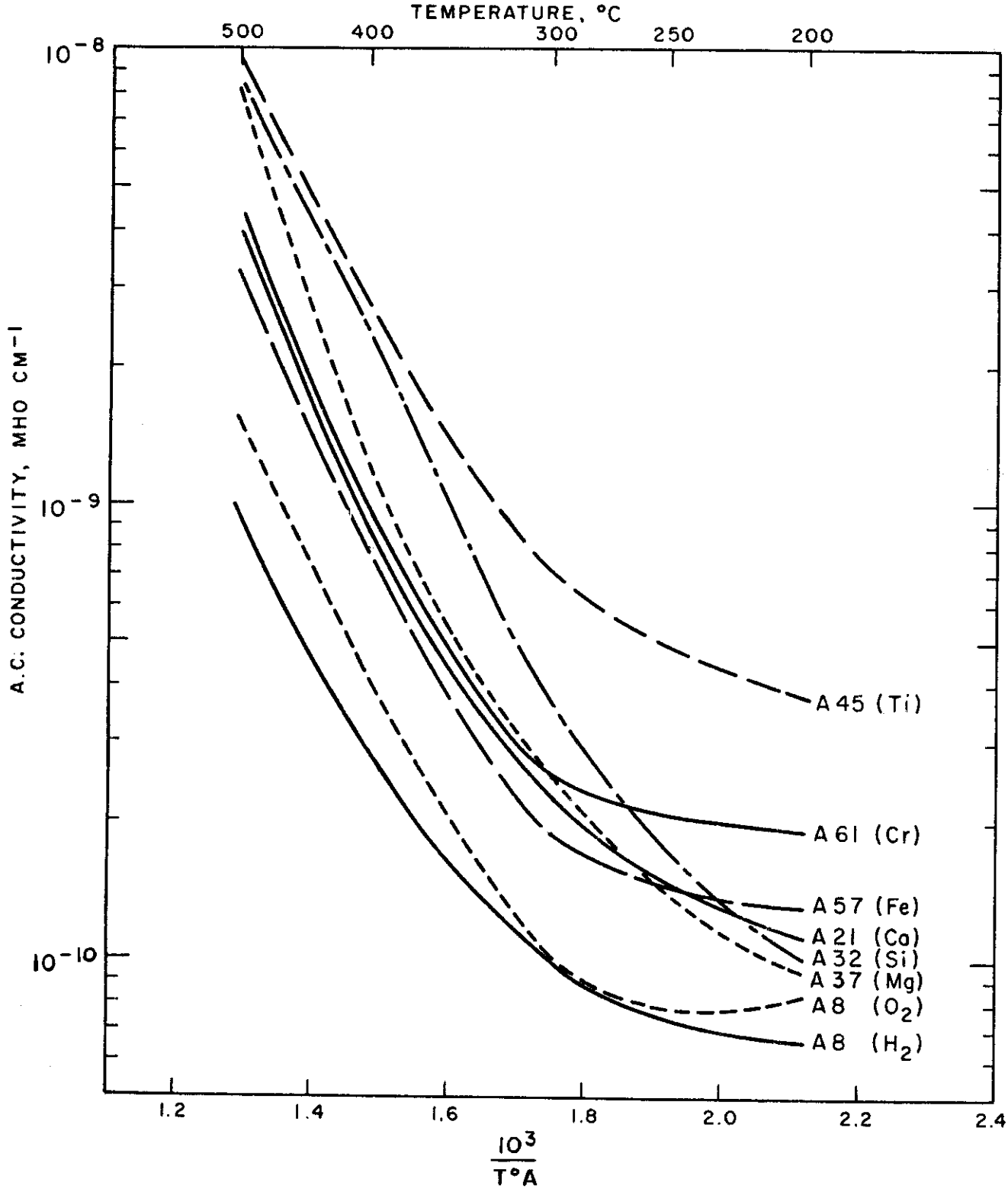

FIG. 11 A.C. CONDUCTIVITIES AT 10^5 C/S OF PURE AND DOPED ALUMINAS.

VI. BIBLIOGRAPHY

1. L. M. Atlas, "Research and Development Services Leading to the Control of Electrical Properties of Materials for High Temperature Radomes" WADC Technical Report 59-300, (October 1959). Contract No. AF 33(616)-5929.

2. J. E. Burke

   (a) "Role of Grain Boundaries in Sintering" J. Am. Cer. Soc. 40, 80-85, (1957).

   (b) "Recrystallization and Sintering in Ceramics," pp. 120-130 in Ceramic Fabrication Processes, W. D. Kingery, Ed., Technology Press of M.I.T. and John Wiley and Sons Inc., New York, (1958).

   (c) "Grain Growth in Ceramics," Chap. 16 in Kinetics of High Temperature Processes," W. D. Kingery, Ed., Technology Press of M.I.T. and John Wiley and Sons, Inc., New York, (1959).

3. L. M. Atlas and R. F. Firestone, "Application of Thermoluminescence and Reflectance Methods to Study of Lattice Defects in Alumina Ceramics" scheduled for publication J. Am. Cer. Soc. 43, (9), (1960).

4. J. Cohen, "Electrical Conductivity of Alumina" Am. Cer. Soc. Bull. 38, (9), 441-446 (1959).

5. C. G. Koops, "Dispersion of Resistivity and Dielectric Constant of Some Semiconductors at Audio Frequencies" Phys. Rev., 83 (1), 121-124, (1951).

6. J. V. Florio, "Dielectric Properties of Alumina at High Temperatures" J. Am. Cer. Soc., 43 (5), 262-267, (1960).

7. R. G. Breckenridge, "Relaxation Effects in Ionic Crystals" Chap. 8 in Imperfections in Ionic Crystals, Eds.: W. Shockley, J. H. Holloman, R. Maurer, and F. Seitz, John Wiley and Sons Inc., New York (1952,) 490 pp.

8. P. O. Johnson, "Statistical Methods in Research" Chap. 14, Prentice-Hall Inc., New York (1949), 367 pp.

9. The characteristics of such capacitors are described by A. R. Von Hippel "Dielectrics and Waves," Chap. 31, John Wiley and Sons Inc., New York (1954), 284 pp.

10. Private communication.

11. E. Yamaka and K. Sawamoto, "Photoinduced Hall Effect in MgO" Phys. Rev., 101, (2), 565-566, (1956).

12. A. R. Hutson, "Semiconducting Properties of Some Oxides and Sulfides" Chap. 13 in Semiconductors, N. B. Hannay, Ed., Am. Chem. Soc. Monograph 140, Reinhold Publishing Corp., New York (1959), 767 pp.

13. J. F. Marshall, M. A. Pomerantz, and R. A. Shatas, "Temperature Dependence of Electron-Bombardment-Induced Conductivity in MgO" Phys. Rev., 106, (3), 432-434, (1957).

14. A. Von Hippel and W. B. Westphal, "High Dielectric Constant Materials as Capacitor Dielectrics, A Study in Dielectric Spectroscopy" Tech. Report 145, Laboratory for Insulation Research, M.I.T., AEC Contract AT(30-1)-1937, NYO 2091,(Dec. 1959.)

15. K. Lichtenecker, "Die Dielektrizitatskonstante naturlicher und kunstlicher Mischkorper" Physik. Zeit. 27, (4/5), 115-118, (1926).

16. Laboratory for Insulation Research, M.I.T., Tech. Report 126, "Tables of Dielectric Materials" VI, 42-43, (June 1958) Contract Nonr-1841 (10).